JOURNAL OF COMPUTATIONAL PHYSICS 112, 12–23 (1994)

Numerical Solution of Stokes Equations with Pressure and Filtration Boundary Conditions

PETER J. SHOPOV AND YURIY I. IORDANOV

Institute of Mathematics, Bulgarian Academy of Sciences, Acad. G. Bontchev Street, bl. 8, 1113 Sofia, P.O. Box 373, Bulgaria

Received August 2, 1990; revised April 27, 1992

A numerical algorithm is presented for two-dimensional Stokes equations (plane and axisymmetric case) with pressure and filtration boundary conditions. The numerical procedure is based on a divergence-free finite element method and is applicable to multiply connected domains. Comparisons between two types of finite elements are performed in order to choose the better one. The numerical method is tested on flows with known numerical and analytical solutions and on different grids. Stress boundary conditions are briefly discussed and compared with pressure ones. The influence of a closely placed outlet on the accuracy of numerical results is studied. Numerical examples are presented, including flow past a system of bodies in a channel, flows in branched channels with or without particles, and in channels of arbitrary shape with filtrating walls. © 1994 Academic Press, Inc.

1. INTRODUCTION

A finite element scheme of divergence-free type is presented for the solution of creeping flow equations for an incompressible fluid in general multiply connected domains. The Stokes equations describe the dynamics of low Reynolds number liquids and thus are applicable to low-scale problems and to viscous media at small velocities. Different types of boundary conditions (B.C.) can be imposed—prescribed velocity (Dirichlet B.C.), prescribed stress, prescribed pressure, filtration (in this order they are described in Section 2 in i, ii, iii, iiii). All possible combinations of these boundary conditions may occur in applications. The latter two types of boundary conditions are more rarely used in numerical modelling and they have been the main object of our interest. In fact these two types of B.C. are variants of a more common type--prescribed tangential velocity and prescribed normal component of stress tensor. A typical feature of such models is that fluxes through one or more parts of the boundary are unknown.

The correctness of the pressure boundary conditions for Stokes equations is proved in [1] and for Navier–Stokes equations in [2], where a numerical example for a flow past a body is also presented. The correctness of the filtration B.C. is proved in [3]. A velocity–pressure finite element method is employed for numerical solution and standard error estimates are obtained in [3].

The pressure B.C. for Navier–Stokes equations are also considered in [4], where an existence and uniqueness result is presented, as well as numerical results for a flow in a right-angle planar branch. A finite difference method of fractional steps type is used. A more complete investigation of this plane problem is given in [5], using a velocity–pressure finite element method (FEM). The pressure B.C. in the context of velocity-pressure FEM are considered in [6]. A finite element numerical method is proposed in [7] for viscoelastic liquid flows with nonstandard B.C., including pressure B.C.

To us only a few investigations are available on the numerical methods for Stokes and Navier–Stokes equations with stress, pressure, and filtration B.C. But in many cases these are more natural than prescribed velocity B.C., especially for internal flows. Such boundary value problems model various processes in engineering, biotechnology, and biomedicine. In this paper we concentrate on the divergence-free approach, which offers some advantages—a relatively small number of unknowns and a positive definite linear system of equations to be solved numerically. Some preliminary information on the subject of this paper is presented in [8]. A related numerical method and some applications are presented in [9–11], but only for Dirichlet B.C. An interesting feature of the numerical method presented is that, although the pressure plays important role in the boundary conditions, it is not directly involved in the numerical scheme.

From a hydromechanical point of view this paper might be considered as a development of [12–14], where a numerical method of finite difference type is proposed for doubly connected domains with Dirichlet B.C. It is based on a coordinate transform of the computational domain into a standard domain consisting of rectangles.

In the case of flows in channels we usually know the pressure drop between both ends but not the velocities. Thus it is more natural to impose pressure B.C. They allow

0021-9991/94 $6.00

a description of the flux through a channel with a particle as a function of the position of the particle and its shape. In [15] the influence of the pressure drop on a single erythrocyte's shape is shown for a fixed but deformable particle in a simply connected domain. The advantages of pressure boundary conditions seem to be even more significant in the unsteady case and for flows driven by pressure pulsation.

Flows in a branched channel, in systems of channels and in devices with many inlets or outlets are important for many engineering applications and in biomedicine, but they have not been studied systematically yet. The relatively low number of investigations here seems to be related to the fact that little attention is payed to nonstandard types of B.C. Studies [4, 5] on a right-angle planar channel were already mentioned. The case when the channel is splitting into two symmetrical branches is considered in [16] for moderate Reynolds numbers using a stream function-vorticity finite difference method. The problem is treated in the half domain, which is simply connected; Dirichlet B.C. are applied. More general cases, when the branches are with different diameters, the enbranchment is not symmetric or otherwise more complicated, and cases of networks of channels and of flows in branched channels in the presence of particles have not been considered yet, as far as we know, even in low Reynolds number approximation.

Flows in the presence of permeable walls are rarely considered, too. In [17] incompressible Navier–Stokes equations are solved in a simply connected domain. Dirichlet, pressure, and filtration B.C. are imposed; the model is in velocity–pressure variables, and a finite volume method is applied for its numerical solution.

2. GOVERNING EQUATIONS

Here we consider the dimensionless form of the 2D stationary Stokes equations for incompressible fluid in a general multiply connected domain Ω with boundary $\Gamma = \partial\Omega$ (see Fig. 1),

$$\operatorname{div} \sigma(\mathbf{v}) + \mathbf{F} = 0 \tag{1}$$

$$\operatorname{div} \mathbf{v} = 0 \tag{2}$$

$$\sigma_{ij}(\mathbf{v}) = -\delta_{ij} p + (\partial_i \mathbf{v}_j + \partial_j \mathbf{v}_i), \tag{3}$$

where $\mathbf{v}$ is the velocity, p is the modified pressure (the physical pressure divided by the viscosity μ), σ is the stress tensor, and $\mathbf{F}$ is the vector of external mass forces.

We consider four types of B.C., supposing $\Gamma = \Gamma_1 \cup \Gamma_2 \cup \Gamma_3 \cup \Gamma_4$, $\Gamma_i = \Gamma_i' \cup \Gamma_i'' \cup \cdots$, $i = 1, 2, 3, 4$ (see Fig. 1 and below).

i. Dirichlet B.C. on Γ_1:

$$\mathbf{v}_{|\Gamma_1} = \mathbf{g}. \tag{4}$$

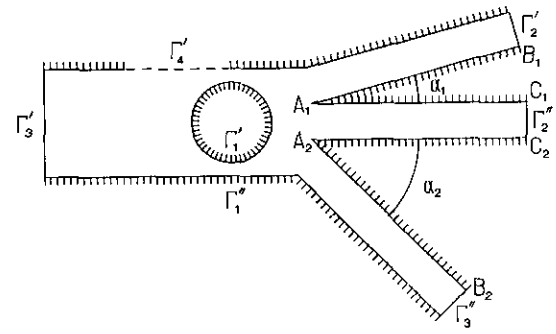

FIG. 1. Principal sketch of the problem with boundary notations.

These B.C. are standard and are usually imposed at rigid channel walls or rigid bodies (particles).

ii. Stress B.C. on Γ_2,

$$-\sigma_{nn|\Gamma_2} = \alpha, \qquad -\sigma_{n\tau|\Gamma_2} = \beta, \tag{5}$$

where n and τ are unit vectors directed to the outward normal and the tangent of Γ_2, respectively. These conditions are applied for flows past bodies at moderate Reynolds numbers in [6].

In the case of a free outlet (inlet), which is supposed to be a segment (e.g., Γ_2', see Fig. 1), when the stress tensor components on Γ_2' are supposed to be as in Poiseuille flow, the right-hand side is taken in the form

$$\alpha(s) = p_{\text{out}}(s); \qquad \beta(s) = 2U_{\max}\, d(s)/b^2, \tag{6}$$

where p_{out} is the external pressure on Γ_2', $2b$ is the width of Γ_2', $d(s)$ is the distance from the point $P(s)$ to the middle of Γ_2', and $U_{\max}$ is the velocity maximum at Γ_2'. The function β could be expressed in terms of the flux Q through Γ_2' as follows:

$$\beta(s) = Qf(s),$$
$$f(s) = \begin{cases} (3/2)\, d(s)/b^3 & \text{plane case} \\ (4/\pi)\, d(s)/b^4 & \text{axisymmetric case.} \end{cases} \tag{7}$$

It is clear from (7) that the function β is not known in advance because the flux Q is unknown. For internal flows this function depends on the solution.

iii. Pressure B.C. on Γ_3:

$$-\sigma_{nn|\Gamma_3} = p_{\text{out}}; \qquad \mathbf{v}_{\tau|\Gamma_3} = 0. \tag{8}$$

For internal flows we impose these B.C. on inlets (outlets) of channels. If the inlet Γ_3' (see Fig. 1) is a segment then (8) is equivalent to:

$$p_{|\Gamma_3'} = p_{\text{out}}; \qquad \mathbf{v}_{\tau|\Gamma_3'} = 0. \tag{9}$$

iv. Filtration B.C. on Γ_4:

$$\mathbf{v}_{n|\Gamma_4} = \gamma(-\sigma_{nn|\Gamma_4} - p_{\text{out}}), \qquad \gamma \geq \gamma_0 > 0;$$
$$\mathbf{v}_{\tau|\Gamma_4} = 0. \tag{10}$$

This is an analogue to Darcy's law—the flux through the boundary is proportional to the pressure drop across it. The B.C. (10) are imposed on permeable walls. The wall thickness is supposed to be small.

Everywhere in this paper in numerical examples p_{out} is supposed to be a constant on each inlet (outlet), which is part of Γ_2, Γ_3, Γ_4.

The existence and uniqueness of the solution of the problem (1)–(10) in $(H^1(\Omega))^2 \times L_2^0(\Omega)$ is proved in [3] (see also the literature therein), where $H^1(\Omega)$ is the corresponding Sobolev space, and $L_2^0(\Omega) = L_2(\Omega) \cap \{f / \int_\Omega f \, d\Omega = 0\}$.

3. NUMERICAL METHOD

The principle of the virtual power for the problem (1)–(10) in the space of divergence-free functions is formulated as

$$a(\mathbf{v}, \delta\mathbf{v}) = \varphi(\delta\mathbf{v}); \qquad \mathbf{v} \in V_g, \qquad \delta\mathbf{v} \in V_0, \tag{11}$$

where $V_g = \{\mathbf{v} / \mathbf{v} \in (H^1(\Omega))^2, \operatorname{div} \mathbf{v} = 0, \mathbf{v}|_{\Gamma_1} = \mathbf{g}, \mathbf{v}_\tau|_{\Gamma_3 \cup \Gamma_4} = 0\}$, in the plane case,

$$a(\mathbf{v}, \delta\mathbf{v}) = \int_\Omega 2\varepsilon_{ij}\, \delta\varepsilon_{ij}\, d\mathbf{x} + \gamma^{-1} \int_{\Gamma_4} \mathbf{v}_n\, \delta\mathbf{v}_n\, ds,$$

$$\varphi(\delta\mathbf{v}) = -\int_{\Gamma_2 \cup \Gamma_3 \cup \Gamma_4} p_{\text{out}}\, \delta\mathbf{v}_n\, ds - \int_{\Gamma_2} \beta\, \delta\mathbf{v}_\tau\, ds + \int_\Omega \mathbf{F}\, \delta\mathbf{v}\, d\mathbf{x},$$

and in the axisymmetric case

$$a(\mathbf{v}, \delta\mathbf{v}) = \int_\Omega (2\varepsilon_{ij}\, \delta\varepsilon_{ij} + (2/r^2)\, \mathbf{v}_r\, \delta\mathbf{v}_r)\, r\, d\mathbf{x} + \gamma^{-1} \int_{\Gamma_4} \mathbf{v}_n\, \delta\mathbf{v}_n\, r\, ds,$$

$$\varphi(\delta\mathbf{v}) = -\int_{\Gamma_2 \cup \Gamma_3 \cup \Gamma_4} p_{\text{out}}\, \delta\mathbf{v}_n\, r\, ds - \int_{\Gamma_2} \beta\, \delta\mathbf{v}_\tau\, r\, ds + \int_\Omega \mathbf{F}\, \delta\mathbf{v}\, r\, d\mathbf{x},$$

where $\varepsilon_{ij} = (\partial_i \mathbf{v}_j + \partial_j \mathbf{v}_i)/2$ and summation is supposed $i = 1, 2$; $j = 1, 2$; and $\mathbf{x} \equiv (x_1, x_2) = (r, z)$, $\mathbf{v} \equiv (\mathbf{v}_1, \mathbf{v}_2) = (\mathbf{v}_r, \mathbf{v}_z)$ in the axisymmetric case.

A finite element method is used for discretization of (11). Two divergence-free finite elements, denoted $Q_2^{(P)}$ and $Q_2^{(Q)}$, will be discussed. They correspond to different initial velocity–pressure elements:

$Q_2^{(P)}$ to Q_2/P_1. Nine-node biquadratic velocity and linear pressure

$$p_h = p_0 + p_1(x_1 - x_1^{(0)}) + p_2(x_2 - x_2^{(0)}), \tag{12}$$

where $x^{(0)} = \frac{1}{4}(x^{(1)} + x^{(2)} + x^{(3)} + x^{(4)})$, $x^{(i)}$-FE vertices;

$Q_2^{(Q)}$ to Q_2/Q_1. The same velocity approximation but a modified one for the pressure

$$p_h = p_0 + p_1 \xi + p_2 \eta, \tag{13}$$

where ξ and η are the local coordinates of the standard reference square $[-1, 1] \times [-1, 1]$.

Following [9], after some transformations we obtain the approximation for velocity in the form

$$\mathbf{v}_h = \sum_{i \in S_1} (u_i \Phi_i^{(u)} + v_i \Phi_i^{(v)} + \psi_i \Phi_i^{(\psi)}) + \sum_{j \in S_2} g_j \Phi_j^{(g)}, \tag{14}$$

where $\{u_i\}$, $\{v_i\}$ are the two velocity components and $\{\psi_i\}$ is the mesh stream function at a set S_1 of vertices of triangulation, and $\{g_j\}$ is the circulation at a set S_2 of finite element sides $\{a_j\}$ (see Fig. 2), where $g_j = c(a_j) \int_{a_j} \bar{\mathbf{v}}_{h,\tau}\, d\gamma$ ($d\gamma = ds$ in the plane case and $d\gamma = r\, ds$ in the axisymmetric one), $c(a_j)$ is a normalizing constant such that $g_j = O(1)$, $\bar{v}_h$ is the initial nine-node biquadratic velocity approximation. Transformations include obtaining the basic functions for the fluxes $\{q_j\}$ at S_2, where $q_j = \int_{a_j} \bar{\mathbf{v}}_{h,n}\, d\gamma$. The difference between $Q_2^{(P)}$ and $Q_2^{(Q)}$ is that $\mathbf{v}_h$ satisfy (15) for $Q_2^{(P)}$ and (16) for $Q_2^{(Q)}$ on any element e of the triangulation:

$$\int_e (\mathbf{x}_s - \mathbf{x}_s^{(0)})(\nabla \cdot \mathbf{v}_h)\, d\Omega = 0, \qquad s = 1, 2, \tag{15}$$

$$\int_e \xi(\nabla \cdot \mathbf{v}_h)\, d\Omega = 0,$$
$$\int_e \eta(\nabla \cdot \mathbf{v}_h)\, d\Omega = 0, \tag{16}$$

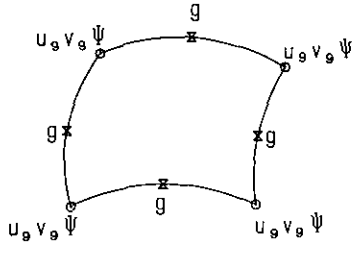

FIG. 2. Finite element employed.

where $d\Omega = d\mathbf{x}$ in the plane case and $d\Omega = r\,d\mathbf{x}$ in the axisymmetric one. Both $Q_2^{(P)}$ and $Q_2^{(Q)}$ satisfy $\int_e \nabla \cdot \mathbf{v}_h\, d\Omega = 0$, so these FE give a divergence-free FE discretization of (11), where pressure unknowns do not take part.

The FE discretization (14) of (11) gives a linear system with a symmetric and positive definite coefficient matrix [3]. After solving it one can calculate the velocity components at the midpoint of every FE side a_j by explicit formulae. If necessary, the pressure can be restored too. For any element e of the triangulation the values of p_1, p_2 can be calculated directly from

$$p_s = -c^{-1}\alpha(\mathbf{v}_h, N_0\mathbf{e}_s), \qquad s = 1, 2 \qquad \text{for} \quad Q_2^{(P)}, \quad (17)$$

$$\begin{pmatrix} p_1 \\ p_2 \end{pmatrix} = -\mathbf{B}^{-1}\begin{pmatrix} \alpha(\mathbf{v}_h, N_0\mathbf{e}_1) \\ \alpha(\mathbf{v}_h, N_0\mathbf{e}_2) \end{pmatrix} \qquad \text{for} \quad Q_2^{(Q)}, \quad (18)$$

where N_0 is the basic function of the central node of e for the standard nine-node biquadratic approximation, $\mathbf{e}_1 = (1, 0)$, $\mathbf{e}_2 = (0, 1)$, $c = \int_e N_0\, d\Omega$, $\mathbf{B}_{2\times 2} = ((\int_e N_0 \nabla\xi\, d\Omega)_{2\times 1}, (\int_e N_0 \nabla\eta\, d\Omega)_{2\times 1})$. The third type of unknowns $\{p_0\}$ of the pressure approximation are restored by a marching procedure. For an arbitrarily initial FE e_0 an arbitrary value of $p_0^{(e_0)}$ is taken. If $p_0^{(\tilde{e})}$ is known and a_j is the common side of $\tilde{e}$ and $\tilde{\tilde{e}}$, then $p_0^{(\tilde{\tilde{e}})}$ is calculated as

$$p_0^{(\tilde{\tilde{e}})} = p_0^{(\tilde{e})} \pm \alpha(\mathbf{v}_h, \Phi_j^{(q)}), \quad (19)$$

and the sign depends on the direction of the parametrization of the side. In this way the pressure may be restored by a marching procedure, including an additive constant. If the pressure takes any part in the B.C. ($\Gamma_2 \cup \Gamma_3 \cup \Gamma_4 \neq \varnothing$) then the value of the additive constant can be determined so that $p_{h|\Gamma_s} = p_{\text{out}}$, $s = 2, 3, 4$.

The numerical method is equivalent to a velocity–pressure finite element method [18, 19]. The standard error estimate [3] holds for the approximate solution $\mathbf{v}_h$, namely,

$$\|\mathbf{v} - \mathbf{v}_h\|_1 + \|p - p_h\|_0 + |R - R_h| \leqslant Ch^2(\|\mathbf{v}\|_3 + \|p\|_2) \quad (20)$$

$$\|\mathbf{v} - \mathbf{v}_h\|_0 + \|\Psi - \Psi_h\|_c \leqslant Ch^3(\|\mathbf{v}\|_3 + \|p\|_2) \quad (21)$$

if $(\mathbf{v}, p) \in (H^3(\Omega))^2 \times (H^2(\Omega) \cap L_2^0(\Omega))$ and $R = \int_{\Gamma_s} \sigma_n\, d\gamma$ is the resistance force on the body with boundary Γ_s, $\|\cdot\|_c$ denotes the *sup*-norm in $C(\Omega)$; $\|\mathbf{v}\|_m$ is the norm in $(H^m(\Omega))^2$, $m = 0, 1, 3$; $\|p\|_m$ is the norm in $H^m(\Omega)$, $m = 0, 2$; where $H^m(\Omega)$, $m = 0, 1, 2, 3$, are the corresponding Sobolev spaces. The proof is based on the abstract theory [20] for the error estimate of Stokes problems.

In the numerical experiments the resistance force is directly calculated by integration over those FE sides which comprise the corresponding body boundary.

4. TESTS AND COMPARISONS

4.1. *Comparison between Two Finite Elements*

In this section we compare the finite elements $Q_2^{(P)}$ and $Q_2^{(Q)}$. The FE Q_2/P_1 is widely used, e.g., [21–23], and is considered the best for Navier–Stokes equations in many applications. The FE Q_2/Q_1 does not seem to be tested directly yet. Kim and Decker [24] compare both FEs in the penalty approach and report that the results for the restored pressure with the Q_2/Q_1 FE are better. Results are reported in [25] which show that $Q_2^{(Q)}$ gives results for the velocity about 30% better than $Q_2^{(P)}$ on the same grids.

The classical exact solution for creeping flow past a sphere from [26] is used as a base of this comparison. If the finite elements are nearly square, both compared elements do not differ essentially, but in the case of considerably deformed elements $Q_2^{(Q)}$ seems to be better. It appears that the $Q_2^{(Q)}$ element is less sensitive to the negative influence of the FE distortion. Here we concentrate on comparisons for the resistance force R on a body, which is often used as a physically natural integral measure for the accuracy of calculations in fluid dynamics (see [22] and references therein). On the other hand, R is the most poorly computed among all basic characteristics of the flow—velocity field, stream lines, pressure distribution, and resistance force.

So, we consider the exact solution for the flow past a sphere [26]. The radius of the sphere is taken as a characteristic length. The problem is treated in a quarter domain, using symmetry conditions in a (r, z) coordinate system. We consider two approximations for the velocity: the FE interpolant of the exact solution on the grid, $\mathbf{v}_{h,I}$, and the numerical solution, $\mathbf{v}_h$. The pressure is restored on the base of $\mathbf{v}_{h,I}$ and $\mathbf{v}_h$, as mentioned in Section 3, and then the resistance force approximations, $R_{h,I}$ and R_h, are computed. Only the layer of finite elements neighboring the body is needed for determining the resistance and we shall denote its thickness in the radial direction by $r_{1,h}$. All grids which are used in our computations are (i) topologically equivalent to a regular grid in the unit square and (ii) uniform in the nonradial direction (N_1 denotes the number of FEs in this direction), but they are rather nonuniform in the radial direction. The grid with $r_{1,h} = 0.25$ has ratios between the first six layers of 1:1:2:2:3:5; the one with $r_{1,h} = 0.10$ has 1:3:5:7:9:11; the one with $r_{1,h} = 0.05$ has 1:2:3:4:5:5; and the one with $r_{1,h} = 0.01$ has 1:2:3:4:6:9. Let N be the number of layers. We shall define a geometrical quantity $\delta = r_{1,h}/(L/N_1)$ as a measure of stretching of FE (here L is the length of the "spherical" part of the boundary). In Table I our results on the comparison and characterization of the two FE are presented. For every grid the first row presents the results for $Q_2^{(P)}$, the second one gives results for $Q_2^{(Q)}$, and the third one gives the ratio $Q_2^{(Q)}/Q_2^{(P)}$ in percents; $\|\cdot\|_c$ and $\|\cdot\|_0$ are discrete analogs (in the nodes of triangulation) of the *sup*-norm and the L_2 norm.

TABLE I

Comparison between $Q_2^{(P)}$ and $Q_2^{(Q)}$ Finite Elements

$r_{1,h}$	N	N_1	δ	$\|\mathbf{v}-\mathbf{v}_h\|_c$	$\|\mathbf{v}-\mathbf{v}_h\|_0$	$\|R-R_h^I\|$	$\|R-R_h\|$
0.25	7	8	1.27	0.000352	0.000140	0.0349	0.0311
				0.000234	0.000107	0.0277	0.0236
				66.48	76.43	79.37	75.88
0.10	7	8	0.51	0.000532	0.000188	0.0192	0.0172
				0.000385	0.000146	0.0102	0.0072
				72.37	77.66	53.13	41.86
0.05	12	8	0.25	0.000381	0.000102	0.0222	0.0160
				0.000158	0.000038	0.0124	0.0056
				41.47	37.25	55.86	35.00
0.01	20	8	0.05	0.000387	0.000095	0.1715	0.0158
				0.000147	0.000030	0.1633	0.0055
				37.98	31.58	94.77	35.09
0.01	20	12	0.08	0.000193	0.000044	0.0369	0.0070
				0.000144	0.000031	0.0323	0.0021
				74.61	70.45	87.53	30.07

The results given in Table I confirm that $Q_2^{(Q)}$ is better. With the decrease of δ, $Q_2^{(Q)}$ gives about as much as 60% better results for the velocity. The deviation on the last grid is probably caused by the error value approaching the accuracy of our computation. The results for the resistance are similar to those for the velocity but only for R_h. With decreasing δ, when $\mathbf{v}_{h,I}$ is used, a considerable deterioration of the pressure restoration causes $R_{h,I}$ to be poorly computed. It seems that the direct usage of the FEM solution to compute the resistance force is not the best way to do it. Perhaps a better result could be achieved by an indirect procedure for determining R that is similar to the one considered in [28] for the Laplace equation, where superconvergence is proved. For the grid with $r_{1,h}=0.01$ and $N_1=8$ the error in pressure estimation is about 33%, so we tested a grid with $r_{1,h}=0.01$ and $N_1=12$. The improvement obtained was considerable for both R_h and $R_{h,I}$, and also for the velocity, although $R_{h,I}$ still remains relatively poorly computed. This shows that cases of significant deviation of δ from one requires some precaution.

Summing up, $Q_2^{(Q)}$ seems to be more promising than $Q_2^{(P)}$. This was confirmed also by our experience with this FE and the Lagrangian finite element method presented in [9]. We employ $Q_2^{(Q)}$ in all further computations.

4.2. *Tests against Known Solutions and Numerical Methods*

First we test our method against the exact Poiseuille solution for the plane flow in a channel and the axisymmetric flow in a tube, respectively. In this case the pressure is constant at the inlet and the outlet. We prescribe it at the inlet and outlet of a channel of unit length and unit half width (a tube of unit length and unit radius) and use four finite elements for a uniform triangulation. As we expected, the numerical solution coincides with the exact one up to the accuracy of the computer arithmetic, because the finite elements are of second order.

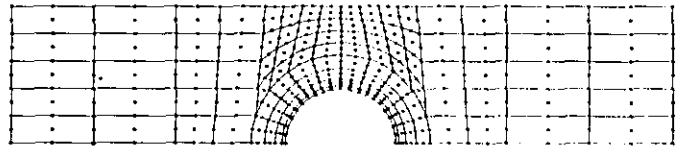

FIG. 3. Example of triangulation.

Further, we consider the flow past a body in a channel in the plane case. We take a centrally situated quiescent cylindrical particle of radius r. Then Ω is symmetric with respect to the channel central line. The problem could be treated in a half domain and falls into the simply connected case. The half of the channel width b is a characteristic length l_{ch}, the length of the channel is l.

It is often difficult to decide how far from the body the "actual infinity" should be placed in order to obtain correct numerical results. Our numerical experience suggests simple criteria whether the inlet (outlet) is placed correctly. We calculate the pressure distribution at the inlet (outlet). If it is not constant with the desired accuracy, then the inlet (outlet) is too close to the body. As a practical rule is used $l \geqslant \max(5b, 12r)$. If $r \leqslant b/3$, results are satisfactory even for $l = 4b$.

We compare the numerical solutions obtained by this method with Dirichlet and pressure B.C. for $r = 0.25b$, $l = 5b$. The employed triangulation is shown in Fig. 3. Two types of problems could be solved—prescribing a parabolic profile for the velocity at the inlet and the outlet of the channel (Problem V), or prescribing the pressures $\tilde{p} + \Delta p$ and $\tilde{p}$, $\Delta p > 0$ (Problem P), and zero tangential velocities. It is easy to see that the numerical solution does not depend on the constant $\tilde{p}$. This has been also confirmed in the numerical experiments.

Take the maximal velocity at the inlet, which is the velocity at the central point A of the inlet, as a characteristic velocity. To obtain the solution $\mathbf{v}_h^{(p)}$ of Problem P, first we find a solution $\tilde{\mathbf{v}}_h^{(p)}$ of Problem P with an arbitrary pressure drop Δp, and then we multiply $\tilde{\mathbf{v}}_h^{(p)}$ with the constant $1/\tilde{\mathbf{v}}_h^{(p)}(A)$ to find the required solution $\mathbf{v}_h^{(p)}$, which corresponds to the pressure drop $\Delta p/\tilde{\mathbf{v}}_h^{(p)}(A)$. Here we essentially use the linearity of the mathematical model for the Stokes case described in Section 2. The solution $\mathbf{v}_h^{(v)}$ of Problem V is directly obtained.

The comparison between both solutions shows good agreement:

$$\|\mathbf{v}_h^{(v)} - \mathbf{v}_h^{(p)}\|_c = \|\mathbf{v}_h^{(v)} - \mathbf{v}_h^{(p)}\|_{c,\text{inlet}} = 0.000260$$

$$\|\mathbf{v}_h^{(v)} - \mathbf{v}_h^{(p)}\|_0 = 0.000070$$

$$\|p_h^{(v)} - p_h^{(p)}\|_{c,\text{inlet}} / \|p_h^{(v)}\|_{c,\text{inlet}} = 0.00585.$$

TABLE II

Horizontal Force on a Quiescent Particle in Poiseuille Flow

r	Faxen	Dvinski and Popel	Present method
0.10	5.7298	—	5.6183
0.15	6.9544	—	6.8935
0.20	8.1304	8.0535	8.0903
0.25	9.2983	9.1673	9.2635
0.30	10.4190	10.3045	10.3768
0.35	11.6074	11.4534	11.5484
0.40	12.7741	12.5727	12.6760
0.45	14.0242	13.7110	13.7822
0.50	15.9348	15.0489	15.1398

Further, we check the accuracy of our algorithm with pressure B.C. against the classical analytical solution of Faxen [29] for a quiescent cylindrical particle in Poiseuille flow. Dvinski and Popel [12] have used this solution to verify their numerical method with Dirichlet B.C. and we present their results, also. In the numerical experiments was taken $l = 6b$. The triangulation used for calculations is similar to the one depicted on Fig. 3. The characteristic pressure and velocity are chosen as

$$p_{ch} = \Delta p\, l_{ch}/(2l) = \Delta p\, b/(2l),$$
$$V_{ch} = p_{ch} l_{ch} = b^2\, \Delta p/(2l), \tag{22}$$

where l is the channel length. In this way we prescribe the dimensionless pressure drop $2l/b$ (Problem P) which would generate unit velocity if there was no particle in the channel. The results are showed in Table II.

Faxen's solution is not exact and loses accuracy with the increase of the diameter of the particle, which explains the growth of the difference between the numerical and the analytical solutions in Table II. It is clear that our results are in good agreement with both other solutions. In Table III the results for several different grids, where M is the total number of FEs in the triangulation are presented; $r_{1,h}$ and δ are the quantities defined in 4.1, F_{app} and F_{Faxen} are the horizontal forces obtained by our method and by Faxen solution, respectively, and $\mathrm{Err} = (F_{app} - F_{Faxen})/F_{Faxen}$ is given in percents. The first row is for the P problem, the second one is for the V problem.

TABLE III

Horizontal Force on a Quiescent Particle $r = 0.3$ in Poiseuille Flow for Different Grids

M	$r_{1,h}$	δ	F_{app}	F_{Faxen}	Err
112	0.025	0.265	10.3768	10.4190	−0.41
			10.4243	10.3846	0.38
240	0.025	0.531	10.4410	10.3889	0.50
			10.3794	10.3546	0.24
458	0.0125	0.265	10.4292	10.5860	−1.48
			10.3038	10.1701	1.31
458	0.0125	0.663	10.3944	10.4018	−0.07

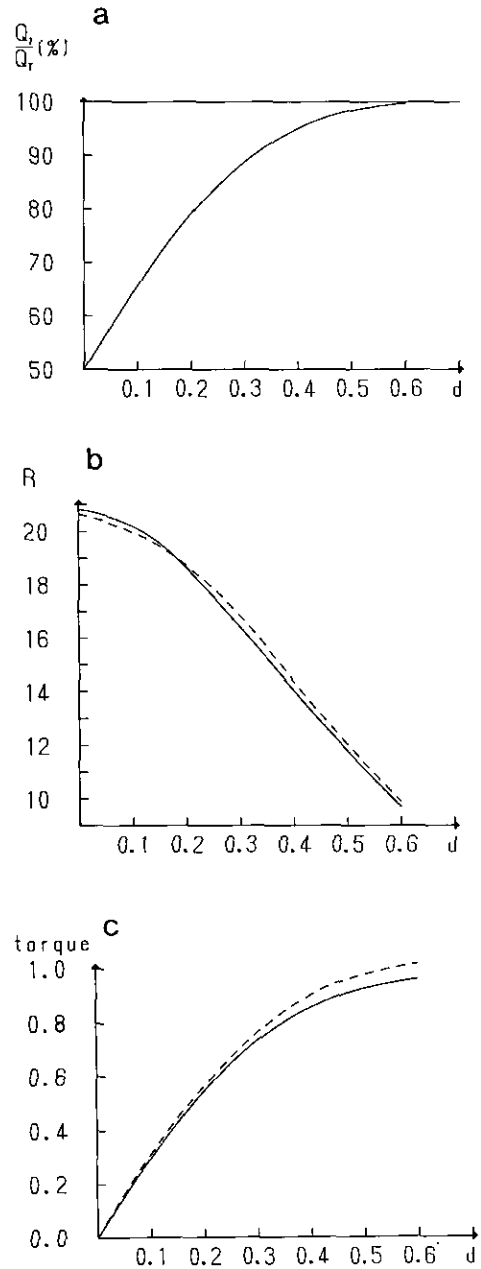

FIG. 4. Flow past an eccentrically placed cylinder $r = 0.3$ in a channel: (a) ratio of the flux through the greater gap Q_1 to the total flux Q_T as a function of the deviation d of the cylinder centroid from the central line of the channel; (b) resistance force as a function of d: (——) present method, (– – –) Dvinsky and Popel [14]; (c) torque as a function of d: (——) present method, (– – –) Dvinsky and Popel [14].

TABLE IV

Comparison between Analytical and Numerical Solution of a Problem with Filtration B.C.

γ	$\|\mathbf{v}\|_c$	$\|\mathbf{v}\|_0$	Err_c	Err_0
0.0001	0.008660	0.006194	0.0013	0.0008
0.001	0.027386	0.018898	0.0049	0.0034
0.01	0.086603	0.053921	0.0523	0.0426
0.1	0.273861	0.136066	0.8311	0.9973
1	1	0.385924	2.4009	3.0516
10	10	2.064722	17.645	32.020

Decreasing $r_{1,h}$ and refining the grid may not improve, but may even deteriorate the results, if δ is small. Only if δ is near one does the numerical solution corresponding to the refined grid seem to be better. This conclusion is like the one in Section 4.1.

We consider also the case of an eccentrically situated quiescent cylindrical particle with the deviation of the particle centroid from the central line of the channel $\measuredangle$. The inlet flux Q_τ gives a characteristic velocity here and Q_1 is the flux through the greater gap between the particle and the walls. We show our results for Q_1 in Fig. 4a and also the results for the horizontal force and the torque, together with those obtained from Dvinski and Popel in [14] in Figs. 4b and c. Again, a good agreement of both presented numerical results can be noted.

Finally, we check the accuracy of the numerical method with filtration B.C. against the analytical solution described in the Appendix for the plane case. The analytical solution is valid in the Stokes case and for $\gamma \ll 1$. We denote $\mathrm{Err}_c = \|\mathbf{v}-\mathbf{v}_h\|_c/\|\mathbf{v}\|_c$ and $\mathrm{Err}_0 = \|\mathbf{v}-\mathbf{v}_h\|_0/\|\mathbf{v}\|_0$, where $\mathbf{v}$ is the analytical solution and $\mathbf{v}_h$ is the numerical one obtained by the presented method. In Table IV both solutions are compared; Err_c and Err_0 are given in percentages.

When γ increases, the validity of the analytical solution diminishes, which explains the growth of the difference between both solutions.

4.3. *Stress B.C. or Pressure B.C.?*

The application of the stress and the pressure B.C. does not differ for the external flows or if the maximal velocity or the flux Q through the inlet (outlet) is known. But the flux Q is not known for the problems discussed here. The function β from B.C. (5) is not known and, hence, the corresponding term does not belong to the right-hand side in (11). If we denote $a_1(\mathbf{v}, \delta\mathbf{v}) = \int_{\Gamma_2} \beta\, \delta\mathbf{v}_\tau\, d\gamma$, $\varphi_1(\delta\mathbf{v}) = -\int_{\Gamma_2\cup\Gamma_3\cup\Gamma_4} p_{\text{out}}\, \delta\mathbf{v}_n\, d\gamma + \int_\Omega \mathbf{F}\, \delta\mathbf{v}\, d\Omega$ from (6), (7), it follows that

$$a_1(\mathbf{v}, \delta\mathbf{v}) = Q \int_{\Gamma_2} f\, \delta\mathbf{v}_\tau\, d\gamma = 2U_{\max} b^{-2} \int_{\Gamma_2} d\, \delta\mathbf{v}_\tau\, d\gamma, \quad (23)$$

and the linear system of Eqs. (24) for (11) will transform into (25) as

$$\mathbf{A}U = F, \quad (24)$$

$$(\mathbf{A} + \mathbf{A}^{(1)})\, U = F^{(1)}, \quad (25)$$

where $\mathbf{A}_{i,j} = a(\Phi_i, \Phi_j)$, $\mathbf{A}^{(1)}_{i,j} = a_1(\Phi_i, \Phi_j)$, $F_j = \varphi(\Phi_j)$, $F^{(1)}_j = \varphi_1(\Phi_j)$, and U is the vector of unknowns. The matrix $\mathbf{A}^{(1)}$ is not symmetric nor positive definite but its elements are of order $O(h)$ while the elements of $\mathbf{A}$ are of order $O(1)$. Hence the symmetry of the system is lost but it is expected that positive definiteness will be preserved, at least for fine meshes.

System (25) can be solved directly but the cost will increase because of the asymmetry. This approach still seems acceptable for the case of Navier–Stokes equations with its natural absence of symmetry, but it is not clear if the additional term (23) deserves so much attention in the Stokes case.

We believe that in our case it is better to keep this term in the right-hand side using an initial guess for Q and then correcting it. If we use iterative methods for the system (24) this will bring about no additional complications, provided that the convergence is not influenced. It is not so expensive to solve the same system with a number of different right-hand sides. For mechanical reasons we expected that such a simple iteration procedure would converge rapidly.

We performed a number of experiments to see how it works. First we considered again Poiseuille flow, and we intentionally used a bad initial guess for $U_{\max}$ to check how it would converge towards its correct value of one. The first one or two iterations smoothed essentially the initial error, see Table V.

Further, we studied the influence of the deviation of the initial guess on the solution for a flow in a branched channel (Fig. 5). The branches are deliberately set short, their lengths are equal to each other and are equal to their widths. The dimensionless pressure at the inlet is 20 and at both outlets it is 10. This problem cannot be solved with Dirichlet B.C. because the fluxes through the outlets are unknown. The problem has been solved in three variants: with pressure B.C. at the inlet and outlets (PPP), with pressure B.C. at the inlet and stress B.C. at the outlets (PSS), only with stress B.C. (SSS), and for different grids (M denotes the total number of FEs in the grid). If there are stress B.C.,

TABLE V

Convergence of the Velocity for Stress B.C.

Case	Iteration 0	1	2	3	4
Plane	0.5	1.05214	0.99479	1.00054	0.99994
Axisymmetric	0.5	1.03573	0.99744	1.00018	0.99998

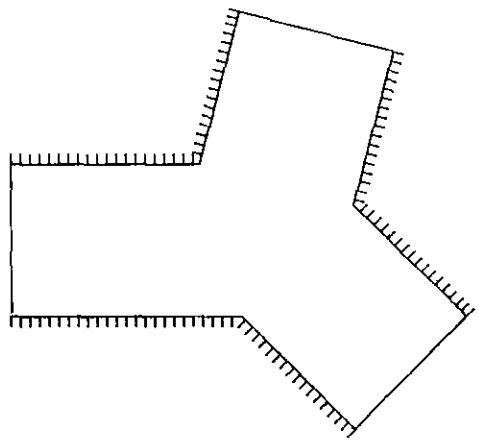

FIG. 5. Geometry of test branched channel.

some iterations are carried out. For any inlet or outlet (where b' is its width) $U^{\max}$ is obtained for the first iteration always by projecting the vector (0, 1), and $U^{\max}$ for the $(k+1)$th iteration is set to $0.75Q^{(k)}/b'$ (according to (6) and (7)). The results are presented in Table VI. The subscript i is for inlet; 1 is for the lower outlet; 2 is for the upper outlet.

The first grid used ($M=20$) was rather coarse and the difference of 2% for the inlet flux Q_i with regard to the finest grid seems acceptable. We want to show that at least for Stokes case the presented method works relatively well on coarse grids.

These experiments confirm that the simple iterative procedure for the case of stress B.C. converges very fast for various geometries. The data presented in Table VI show that solutions of PPP, PSS, and SSS problems are very close if the grid is the same (the difference between fluxes is less than 0.1%). So the stress B.C. does not seem to be essentially better than the pressure ones for the Stokes equations and, thus, there is no payoff for the mentioned numerical complications in the case of stress B.C.

To support this conclusion, we performed a comparison between velocity, pressure, and stress B.C., using the resistance force as an integral measure for the accuracy of the solution. We considered once again the flow past a centrally situated quiescent cylinder in a channel for $r=0.25b$, $l=l_{in}+l_{out}$, where l_{in} (l_{out}) is the length between the inlet (outlet) and the particle centroid (see also the notation in Section 4.2). If $l_{in}=2.4$, according to Section 4.2, the inlet is placed far enough from the body to apply correctly velocity B.C. The maximal velocity at the center line is chosen as the characteristic velocity. We applied velocity, pressure, and stress B.C. at the outlet and varied the distance l_{out}. From Table II we knew the value of the resistance force well enough. In this way we compared the sensitivity of the three kinds of B.C. to the truncation of the computational domain past the body. The results are presented in Table VII. The triangulation used is similar to the one presented on Fig. 3, but the FEs at the outlet zone are made shorter.

The error in resistance $\mathrm{Er}_r^{(\alpha)}$ is defined as $(R^{(\alpha)}-R^{(ex)})/R^{(ex)}$ (given in percentages) and $R^{(ex)}$ is calculated on the base of Faxen's solution; the upper index α is v, p, or σ for velocity, pressure, or stress B.C.; the maximum of the module of the velocity at the outlet is $V_m^{(\alpha)}$; the deviation of the point where $V_m^{(\alpha)}$ is achieved from the central line is $d_m^{(\alpha)}$; the maximum of the tangential velocity at the outlet is $V_{\tau,m}^{(\alpha)}$, and the velocity at the central point at the outlet is $V_c^{(\alpha)}$.

As we expected, the velocity B.C. yield poor results if the outlet is placed closer than four particle radii from the body, and the error grows very fast. The pressure and stress B.C. are better and both display a comparable accuracy. Even though the zero tangential velocity condition is clearly unphysical the pressure B.C. give the best results for all values of l_{out}.

The general conclusion from these results is that the stress B.C. should be used only if the pressure B.C. seems to be clearly unfit for the considered problem.

TABLE VI

Comparison of Different B.C. for Flow in Branched Channel

M		Q_i	Q_1	Q_2	$(Q_i/Q_i^{\max})\times 100\%$	$(Q_1/Q_i)\times 100\%$
20	PPP	1.5026	0.7866	0.7160	98.09	52.35
	PSS[1]	1.5036	0.7760	0.7276		
	PSS[2]	1.5021	0.7867	0.7153	98.05	52.37
	SSS[1]	1.5083	0.7785	0.7298		
	SSS[2]	1.5030	0.7873	0.7158		
	SSS[3]	1.5032	0.7869	0.7163	98.13	52.35
80	PPP	1.5257	0.7873	0.7384	99.60	51.60
	PSS[1]	1.5270	0.7760	0.7510		
	PSS[2]	1.5251	0.7878	0.7373	99.56	51.66
	SSS[1]	1.5314	0.7785	0.7529		
	SSS[2]	1.5249	0.7878	0.7371		
	SSS[3]	1.5251	0.7874	0.7377	99.56	51.63
160	PPP	1.5319	0.7862	0.7457	100.00	51.32

TABLE VII

Comparison of Resistance for Velocity, Pressure, and Stress B.C.

l_{out}	Er_r^v	Er_r^p	Er_r^σ	V_m^p	V_m^σ	d_m^p	d_m^σ	$V_{\tau,m}^\sigma$	V_c^p	V_c^σ
2.4	−0.38	−0.38	−0.38	1.00	1.00	0.0	0.0	−0.00	1.00	1.00
1.5	−0.36	−0.38	−0.41	0.97	0.97	0.0	0.0	−0.03	0.97	0.97
1.0	1.12	−0.50	−1.37	0.84	0.84	0.4	0.4	−0.15	0.77	0.78
0.7	11.44	−2.61	−6.33	0.97	0.93	0.6	0.6	−0.30	0.39	0.45
0.5	51.28	−8.90	−14.88	1.14	1.06	0.6	0.6	−0.37	0.07	0.20

5. SAMPLE APPLICATIONS

The particular applications of the method discussed in the paper are of three kinds. We consider first a flow past a system of bodies in a channel at a given pressure drop. Here numerical results are presented for two particles but the method is as well applicable to a greater number of particles. Such problems are important for the theory of suspensions, flows of erythrocytes in capillaries, hemorheology, and for heat–mass exchangers. The second kind of applications includes flows in branched channels and channel networks, with or without particles, driven by pressure drops. Such problems are related to, e.g., blood flow through microvessels. The third kind includes flows in channels or tubes of arbitrary shape and with filtrating walls, which are related to, e.g., ultrafiltration technology. In all cases considered below the flux through the inlet, the outlet, or the permeable wall is not known.

There are a number of numerical examples of flows past a system of fixed bodies with Dirichlet B.C. at the "inlet" in an infinite liquid, e.g., a nest of cylinders [24], modelling a heat exchanger in a nuclear reactor, or wings [23], related to a section of a turbomachine. As far as we know, such problems have not been studied in a channel.

A flow past two cylinders in a channel is presented in Fig. 6. Only the half-domain is depicted because of the symmetry of the problem. The channel half-diameter is chosen as a characteristic length. The radii of the particles B_1 and B_2 are equal to 0.2 and the distances of their centroids from the upper wall W_1 are $d_1 = 0.5$, $d_2 = 1.2$. The channel length is $l = 3$ and the pressure B.C. are used at the inlet and the outlet with pressure drop $\Delta p = 6$, which corresponds to the actual channel length and the formulae (22). The total flux through the channel is 13.21% from the one in the same channel without particles. The flux through the first gap is $Q_{W_1B_1} = 0.0240$ (width $w = 0.3$, $Q_{W_1B_1}/Q_{W_1W_2} = 13.63\%$). This is relatively less than in the second one $Q_{B_1B_2} = 0.0365$ (width $w = 0.3$, $Q_{B_1B_2}/Q_{W_1W_2} = 20.73\%$), due to the influence of the wall. The flux through the third gap is $Q_{B_2W_2} = 0.1156$ (width $w = 0.6$, $Q_{B_2W_2}/Q_{W_1W_2} = 65.64\%$), which is much greater than the previous ones when related to unit length ($2Q_{W_1B_1}/Q_{B_2W_2} = 41.52\%$, $2Q_{B_1B_2}/Q_{B_2W_2} = 63.15\%$). This is due to the interaction of both bodies as a whole with the flow. They play the role of one complex obstacle in the channel and the main flow goes under them. As might be expected, the maximum of the velocity at the gaps between the particles and walls is closer to the body, due to its round shape, and at the middle it is at the gap between both bodies. The resistance force at the first particle, $R_1 = 1.8279$, is smaller than at the second one, $R_2 = 2.1258$, as well as the torques $T_1 = 0.00372$, $T_2 = 0.09320$, because the flow is stronger at the central region. The flow exerts a force that tends to rotate both particles in an anticlockwise direction.

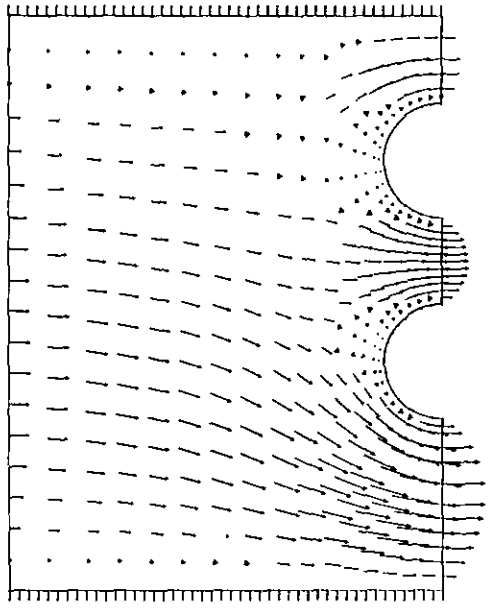

FIG. 6. Flow past two bodies in a channel.

Three examples of flows in branched channels are presented next. In all cases the characteristic length is the half-diameter of the root channel and the length needed for the definition of the characteristic pressure (22) is the sum of the length of the root part l_r and of one branch l_b, where l_r is measured from the inlet of the channel to the junction point (or points), l_b is measured from the junction point to the end of the branch (e.g., $l_{b1} = A_1B_1$, $l_{b2} = A_1C_1 = A_2C_2$, $l_{b3} = A_2B_2$; see Fig. 1). All branches are taken with the same length and diameter d_b, and with equal pressure $p_{out} = 0$ at their outlets, but the junction angles with the root part (e.g., $\alpha_{b1} = \alpha_1$, $\alpha_{b2} = 0$, $\alpha_{b3} = \alpha_2$; see Fig. 1) vary.

First we consider a flow in a triply branched channel with $l_r = 5$, $l_b = 4$ ($\Delta p = 18$), $d_b = \frac{2}{3}$, and the junction points lying at lines parallel to the center line of the channel at distances $\frac{2}{3}$ from the nearer wall. The middle branch Br_2 is a horizontal one, the upper one Br_1 joins with angle α_1, which varies, and the lower one Br_3, with $\alpha_3 = 45°$. Pressure B.C. is applied at the inlet and the outlets, and the results are presented in Figs. 7a, b. The maximal total flux through the channel $Q_T^{max} = 0.2974$ is achieved for $\alpha_1 = 90°$ which is again only 22.31% of the flux in a simple channel with the same length. In general, the influence of the junction angle α_1 is not great for Stokes flows. In this case the distance which the fluid runs is a more decisive factor than the disposition of the branches with respect to the central line of the channel. For the end branches the way of measuring l_b determines a decrease of the integral distance from the inlet that is proportional to the increase of the junction angle. As can be seen in Fig. 7a, for $\alpha_1 > 30°$ the flux through Br_1 is already greater than the one through the middle

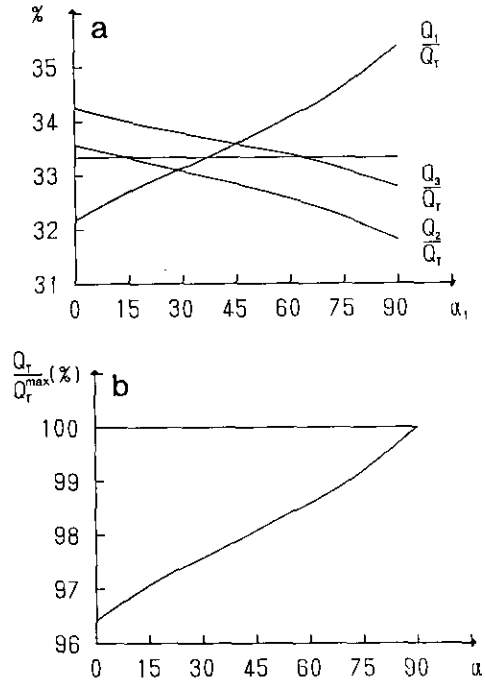

FIG. 7. Flow in a triply branched channel: (a) ratios of the fluxes Q_1, Q_2, Q_3 through the branches to the total flux Q_T as functions of junction angle α_1; (b) ratio of the total flux Q_T to the maximal total flux $Q_T^{\max}$ (for $\alpha_1 = 90°$) as a function of α_1.

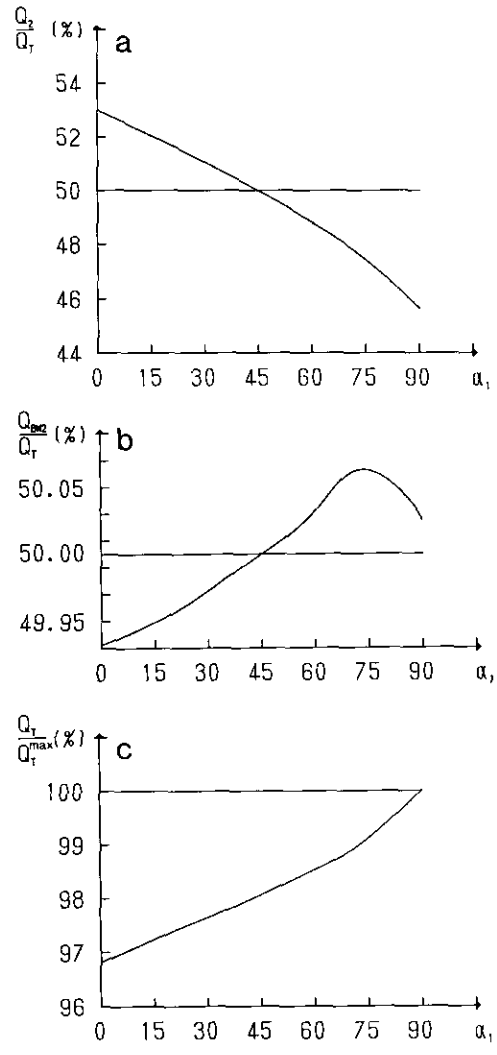

FIG. 8. Flow past a rigid body in a branched channel: (a) ratio of the flux Q_2 through the branch with fixed junction angle $\alpha_2 = 45°$ to the total flux Q_T as a function of junction angle α_1; (b) ratio of the flux Q_{BW2} through the gap between the wall of the branch with fixed junction angle and the rigid body to the total flux Q_T as a function of α_1; (c) ratio of the total flux Q_T to the maximal total flux $Q_T^{\max}$ (for $\alpha_1 = 90°$) as a function of α_1.

branch—the influence of the wall in the root part of the channel is compensated by the decrease of the integral distance for Br_1.

We consider as a second example the flow past a centrally situated cylinder in a branched channel, $l_r = 5$, $l_b = 3$ ($\Delta p = 16$), $d_b = 1$, the junction point being at the center line of the channel, $r_{cyl} = 0.5$, the distance from the particle centroid to the inlet equal to 3; angle α_1 varies and $\alpha_2 = 45°$. This is a natural generalization of problems for flows past a body in a channel [26]. Our results are presented on Figs. 8a, b, c. Now the maximal total flux through the channel $Q_T^{\max} = 0.2352$ and again it is obtained for $\alpha_1 = 90°$. Figure 8a confirms the general conclusion for Stokes flows that the distance which the fluid runs is more important than the disposition of the branches. The hydrodynamic interaction of the particle with the branches is weak, as Fig. 8b shows us. It is interesting that the flux Q_{BW2} through the gap between the wall of Br_2 and the particle is always less (greater) than half of the total flux Q_T, when the flux Q_2 through Br_2 is greater (less) than half of Q_T. The slope of the graph in Fig. 8b is reversed when $\alpha < 75°$, compared to the one in Fig. 8a. Indeed, the scale of the graph in Fig. 8b is 50 times smaller than the one in Fig. 8a, but the accuracy of our method is great enough to assure that this result is not caused only by numerical noise.

A natural development of the problem is to investigate the motion of a drop in a branched channel, which is also a simple model for a flow of an erythrocyte in a microvessel. For solving of this Navier–Stokes problem we use the method, presented in [9], which is based on a Lagrangian approach, a fully implicit time scheme, and a mesh redefinition procedure. Once again, pressure B.C. are used at the inlet and at the outlets. The pressures are $p_{\text{inlet}} = 2$, $p_{B1} = 0$, $p_{B2} = 1$, where $B1$ is the upper branch and $B2$ is the lower one. The Reynolds number of the suspended fluid is $\text{Re}_s = 10$ and that of the drop $\text{Re}_d = 1$. The Weber number of the free boundary is $\text{We} = 3$. In Fig. 9 the state of the drop is pictured at several times.

Finally, we consider a flow in a tube with filtration through the walls and with a rigid, centrally placed spheri-

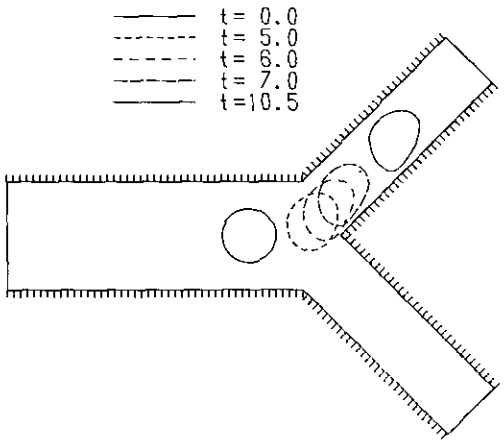

FIG. 9. Pressure-driven motion of a drop in a branched channel.

cal particle. The tube has three parts—cylindrical parts with rigid walls at the ends and a conical part with permeable walls in the middle. Every part has unit length in the central line direction; the radii are $r_{\text{inlet}} = 1$, $r_{\text{outlet}} = 0.5$. The particle radius is $r_{\text{part}} = 0.5$ and the distance between the inlet and the particle center in the central line direction is $d = 1.5$. A characteristic pressure is chosen according to (22), where $l = 3$, but the constant 2 in (22) has to be replaced by 4 in the axisymmetric case, and then $\Delta p \equiv p_{\text{inlet}} - p_{\text{outlet}} = 12$ for the dimensionless pressure. The flow for $\gamma = 0.01$ and $p_{\text{inlet}} = 12$, $p_{\text{outlet}} = 0$, $p_{\text{filtr}} = 6$ is presented on Fig. 10. The total flux through the narrowing tube with filtrating part without particles is 26.38% from the flux in a cylindrical tube with unit radius, with rigid walls and without particles, and 11.70% if there is a particle with shape, size, and displacement as was described. The loss in the flux through the filtration part of the wall is 53.70% and 84.38% of the total flux in the first case and in the second case, respectively, although the permeability of the filtration part is small and, even in the second case, there is a weak influx through a portion of the filtrating walls (see Fig. 10), so there is an outflux only through part of the filtrating walls. These results suggest again the general conclusion for Stokes flows that the distance which the fluid runs is a rather decisive factor. Here this factor influences more than the permeability of the walls. The presence of the particle only amplifies the flux through the filtration part of the walls.

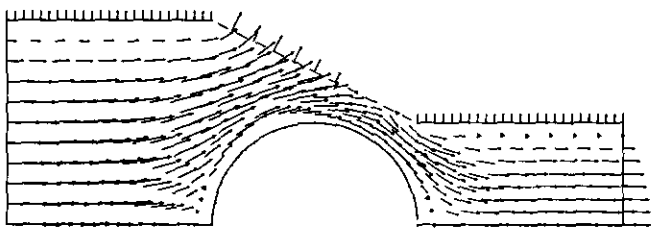

FIG. 10. Flow past a rigid body in a narrowing tube with filtration through the walls.

6. CONCLUSIONS

In this paper we propose a finite element algorithm of divergence-free type for Stokes equations with pressure, stress, and filtration boundary conditions, which is equally applicable to simply and multiply connected domains. It is typical for the considered problems that the flux through parts of the boundary is unknown. The tests for comparability with known solutions, as well as the existing error estimates, prove that the treatment of the mentioned problems with our method yields no more complications than in the case of standard Dirichlet B.C. On the other hand, such boundary conditions are more natural for many mechanical and engineering problems.

Some experiments are also performed with stress B.C. They show good agreement with results obtained by the application of pressure B.C. Usually stress B.C. are considered to yield more exact results than pressure B.C. because the first are more flexible at the outlets. The results presented here do not confirm such an opinion in the case of Stokes equations—both types of B.C. yield approximately the same accuracy and which type of them is better depends much on the problem.

We present some numerical examples to create an idea for the scope of possible areas of application of this method. Our main objective is to develop a divergence-free numerical method for general Navier–Stokes equations in domains with both fixed and free boundaries with imposed pressure and filtration B.C., having in mind a wider field of applications, e.g., viscous cavitation or capillary motion in tubes with dynamic contact lines. We hope to present numerical examples for moderate Reynolds numbers in a following paper.

APPENDIX

The analytical solution for the flow in an infinite channel (only with an inlet) with permeable walls for the plane case can be obtained. Because of symmetry of the problem we solve it in a half domain.

Let $\Omega = \{(x, y)/x > 0,\ y \in (0, H),\ H > 0\}$, $\partial\Omega = \Gamma' \cup \Gamma'' \cup \Gamma_4$ where $\Gamma' = \{(x, H)/x \geqslant 0\}$, $\Gamma'' = \{(0, y)/y \in (0, H)\}$, $\Gamma_4 = \{(x, 0)/x \geqslant 0\}$ (location of filtration B.C.) and $\mathbf{v} = (u, v)$. We suppose that $p = p(x)$ and neglect the terms $\partial^2_{xx} u$, $\partial^2_{xx} v + \partial^2_{yy} v$, which is correct if $\gamma \ll 1$, as will be explained below. Then Eqs. (1)–(3) are equivalent to

$$dp/dx = \partial^2_{yy} u, \qquad \partial_x u + \partial_y v = 0.$$

If $p_{\text{out}|\Gamma_4} = \text{const}$ and dimensionless pressure is defined as $p^* = (p - p_{\text{out}})/p_{\text{ch}}$, then the B.C. on Γ_4 take the form

$$u_{|\Gamma_4} = 0, \qquad v_{|\Gamma_4} = -\gamma p.$$

Solution of the problem can be obtained with the B.C. on Γ' and Γ'' as

$$\partial_y u_{|\Gamma'} = 0, \qquad v_{|\Gamma'} = 0,$$
$$p_{|\Gamma''} = p(0) = p_0,$$

and assuming that the solution is bounded at infinity. Then it is given by

$$u(x, y) = -\tfrac{1}{2} p_0 (3\gamma/H^3)^{1/2} \exp(-(3\gamma/H^3)^{1/2} x) \times (y^2 - 2Hy),$$
$$v(x, y) = -\tfrac{1}{6} p_0 (3\gamma/H^3) \exp(-(3\gamma/H^3)^{1/2} x) \times (y^3 - 3Hy^2 + 2H^3).$$

It can be shown that $\partial^2_{xx} u = O(\gamma^{3/2})$, $\partial_{xx} v^2 + \partial_{yy} v^2 = O(\gamma)$ and neglecting them is correct for $\gamma \ll 1$. For numerical experiments the domain $\Omega' = \Omega \cap \{(x, y)/x \leqslant 2\}$ is considered and $H = 1$, $p_0 = 1$ are taken.

ACKNOWLEDGMENTS

This work was supported by Grant No. 55-26-3-1987 from the Bulgarian Ministry of Science and Higher Educations. The authors thanks Professor R. D. Lazarov and K. Beronov for reading the manuscript and providing helpful comments.

REFERENCES

1. O. Pironneau, *C.R. Acad. Sci. Paris Ser. I* **303**, 403 (1986).
2. C. Begue, C. Conca, F. Murat, and O. Pirronneau, *C.R. Acad. Sci. Paris Ser. I.* **304**, 23 (1987).
3. P. J. Shopov, *C.R. Acad. Bulgar. Sci.* **42**, 33 (1989).
4. B. G. Kuznetchov, N. P. Moshkin, and Sh. Smagulov, in *Numerical Methods for Dynamics of Viscous Liquid*, (Novosibirsk, Moscow, 1985), p. 188. [Russian]
5. R. E. Hayes, K. Nanddacumar, and H. Nasr-El-Din, *Comput. Fluids* **17**, 537 (1989).
6. P. Gresho and R. Sani, *Int. J. Numer. Methods Fluids* **7**, 1111 (1987).
7. Chr. Scheurer, Akademie der Wissenschaften der DDR, Institut für Mechanik, Report 22, Karl-Marx-Stadt, 1989. [German]
8. P. J. Shopov and Y. I. Iordanov, in *Proceedings, VI National Congress of Theoretical and Applied Mechanics, Varna, Bulgaria, 1989;* (Publ. House Bulgar. Acad. Sci., Sofia, 1990), Vol. 3, p. 342.
9. P. J. Shopov, P. D. Minev, and I. B. Bazhlekov, *Int. J. Numer. Methods Fluids* **14**, 681 (1992).
10. I. B. Bazhlekov and P. J. Shopov, *C.R. Acad. Bulgar. Sci.* **43**, 9 (1990).
11. P. J. Shopov, P. D. Minev, I. B. Bazhlekov, and Z. Zaprianov, *J. Fluid Mech.* **219**, 241 (1990).
12. A. S. Dvinski and A. S. Popel, *J. Comput. Phys.* **67**, 73 (1986).
13. A. S. Dvinski and A. S. Popel, *Comput. Fluids* **15**, 391 (1987).
14. A. S. Dvinski and A. S. Popel, *Comput. Fluids* **15**, 405 (1987).
15. P. R. Zarga, S. Chien, and R. Skalak, in *Computational Methods for Fluid-Structure Interaction Problems*, edited by T. Belitschko and T. L. Geers (Am. Soc. Mech. Eng., ASME, AMD V26, New York, 1977), p. 65.
16. J. S. Brambey and D. S. Sloan, *Comput. Fluids* **15**, 297 (1987).
17. R. Albanese, F. Grasso, and C. Meola, in *Proceedings, Fifth International GAMM Conference on Numerical Methods in Fluid Mechanics, Rome, Italy* (Springer-Verlag, New York/Berlin, 1983).
18. P. S. Shopov, *Serdica* **10**, 198 (1984). [Russian]
19. C. Cuvelier, A. Segal, and A. A. van Steenhoven, *Finite Element Methods and Navier–Stokes Equations* (Reidel, Dordrecht, 1986).
20. V. Girault and P.-A. Raviart, *Finite Element Approximation of the Navier–Stokes Equations*, Lecture Notes in Mathematics, Vol. 749 (Springer-Verlag, New York/Berlin, 1979).
21. M. S. Engelman, R. L. Sani, P. M. Gresho, and M. Bercovier, *Int. J. Numer. Methods Fluids* **2**, 25 (1982).
22. K. A. Cliffe and D. A. Lever, *J. Comput. Phys.* **62**, 321 (1986).
23. A. Fortin, M. Fortin, and J. J. Gervais, *J. Comput. Phys.* **70**, 295 (1987).
24. S.-W. Kim and R. Decker, *Int. J. Numer. Methods Fluids* **9**, 43 (1989).
25. P. D. Minev and P. J. Shopov, in *Proceedings, XV Nat. Summer School, Numerical Methods and Applications, Varna, 1989* (Publ. HES "V. Lenin," Sofia, 1990).
26. J. Happel and H. Brenner, *Low Reynolds Number Hydrodynamics* (Prentice–Hall, Englewood Cliffs, NJ, 1965).
27. P. J. Shopov, Ph.D. thesis, Bulgarian Academy of Sciences, 1986 (unpublished).
28. R. D. Lazarov, A. I. Pehlivanov, S. S. Chow, and G. F. Carey, Preprint 08-1989, Enhanced Oil Recovery Institute, University of Wyoming, 1989.
29. H. Faxen, *Proc. R. Swedish Inst. Eng. Res. (Stockholm)* **187**, 1 (1946).